

## Electronic Supplementary Information

### Benzene-cored AIEgens for deep-blue OLEDs: high performance without hole-transporting layers, and unexpected excellent host for orange emission as a side-effect

Xuejun Zhan, <sup>‡</sup><sup>1</sup> Zhongbin Wu, <sup>‡</sup><sup>2</sup> Yuxuan Lin,<sup>1</sup> Yujun Xie,<sup>1</sup> Qian Peng,<sup>3</sup> Qianqian Li,<sup>1</sup> Dongge Ma,<sup>\*2</sup> and Zhen Li<sup>\*1</sup>

<sup>1</sup> Department of Chemistry, Wuhan University, <sup>2</sup> Changchun Institute of Applied Chemistry, The Chinese Academy of Sciences, <sup>3</sup> Institute of Chemistry, The Chinese Academy of Sciences.

<sup>‡</sup> The authors contributed equally to this work.

### Table of Contents

**Chart S1.** Chemical structures of the previous deep-blue luminogens.

**Chart S2.** Synthetic routes of the synthesis of TPA-CN-TPA.

**Chart S3.** Chemical structures of Ph<sub>3</sub>TPE and Ph<sub>2</sub>TPE.

**Scheme S1.** Chemical structures and synthetic routes of the previous four luminogens.

**Figure S1.** DSC curves of the four luminogens recorded under N<sub>2</sub> at a heating rate of 10 °C/min. (A: 2TPA-CN; B: 3TPA-CN; C: 2TPE-CN; D: 3TPE-CN)

**Figure S2.** PL spectra of 2TPA-CN (A) and 3TPA-CN (B) in various solvents (~10 μM).

**Figure S3.** UV-vis spectra of 2TPA-CN (A) and 3TPA-CN (B) in various solvents (~10 μM).

**Figure S4.** Calculated UV spectrum of 2TPE-CN.

**Table S1.** Absorption wavelengths and oscillator strength of 2TPE-CN evaluated by the TD-DFT (CAM-B3LYP/6-31G (d)) calculation.

**Figure S5.** Calculated UV spectrum of 3TPE-CN.

**Table S2.** Absorption wavelengths and oscillator strength of 3TPE-CN evaluated by the TD-DFT (B3LYP/6-311G (d, p)) calculation.

**Figure S6.** PL spectra of the films.

**Figure S7.** PL spectra of **2TPA-CN** (A) and **3TPA-CN** (B) in THF/cyclohexane mixtures with different cyclohexane fractions. Concentration:  $\sim 10 \mu\text{M}$ .

**Figure S8.** Quantum yields of **2TPA-CN** and **3TPA-CN** in THF/cyclohexane mixtures with different cyclohexane fractions.

**Figure S9.** (A) PL spectra of **2TPE-CN** in THF/H<sub>2</sub>O mixtures with different water fractions ( $f_w$ ). (B) Plots of fluorescence quantum yields determined in THF/H<sub>2</sub>O solutions using 9,10-diphenylanthracene ( $\Phi = 90\%$  in cyclohexane) as standard versus water fractions. Inset in (B): photos of **2TPE-CN** in THF/water mixtures ( $f_w=0$  and 99%) taken under the illumination of a 365 nm UV lamp.

**Figure S10.** Luminescence (L) and phosphorescence (P) spectra of **2TPA-CN** and **3TPA-CN** at 77 K in a frozen 2-methyl-THF matrix. Concentration:  $\sim 10^{-3} \text{ M}$ .

**Figure S11.** Emission decay of the four luminogens in oxygen-free toluene solution at room temperature.

**Figure S12.** Cyclic voltammograms recorded in dichloromethane.

**Figure S13.** (A) Power efficiency-luminance characteristics and (B) External quantum efficiency-luminance characteristics of the four luminogens. Device configurations: ITO / MoO<sub>3</sub> (10 nm) / NPB (60 nm) / mCP (15 nm) / X (30 nm) / TPBi (30 nm) / LiF (1 nm) / Al.

**Figure S14.** EL spectra of EL devices at different applied voltages of **2TPA-CN** (A), **3TPA-CN** (B), **2TPE-CN** (C) and **3TPE-CN** (D). Device configurations: ITO / MoO<sub>3</sub> (10 nm) / NPB (60 nm) / mCP (15 nm) / X (30 nm) / TPBi (30 nm) / LiF (1 nm) / Al.

**Figure S15.** (A) Current density-voltage-luminance characteristics, (B) Power efficiency-luminance characteristics and (C) EL spectra of EL device at different applied voltages. Device configurations: ITO / MoO<sub>3</sub> (10 nm) / **3TPA-CN** (70 nm) / TPBi (30 nm) / LiF (1 nm) / Al.

**Figure S16.** (A) Current density-voltage-luminance characteristics, (B) Power efficiency-luminance characteristics and (C) External quantum efficiency-luminance characteristics. Device configurations: ITO / MoO<sub>3</sub> (10 nm) / NPB (60 nm) / mCP (10 nm) / BmPyPb: x% **3TPA-CN** (20 nm) / BmPyPb (10 nm) / TPBi (35 nm) / LiF (1 nm) / Al.

**Figure S17.** EL spectra of doped devices at different applied voltages. Device configurations: ITO / MoO<sub>3</sub> (10 nm) / NPB (60 nm) / mCP (10 nm) / BmPyPb: x% **3TPA-CN** (20 nm) / BmPyPb (10 nm) / TPBi (35 nm) / LiF (1 nm) / Al. (A: 30%; B: 40%; C: 50%)

**Figure S18.** (A) Current density-voltage-luminance characteristics, (B) Power efficiency-luminance characteristics and (C) EL spectra of the device with CBP as the host. Device configurations: ITO / MoO<sub>3</sub> / NPB (60 nm) / mCP (10 nm) / CBP:PO-01 (20 nm, 10 wt%) / TPBI (40 nm) / LiF (1 nm) / Al.

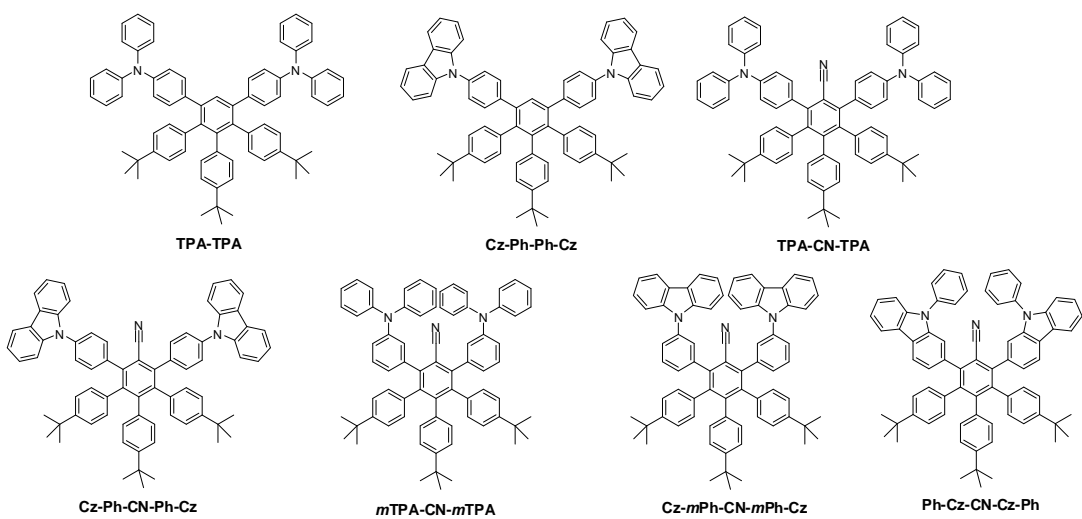


**Chart S1.** Chemical structures of the previous deep-blue luminogens.

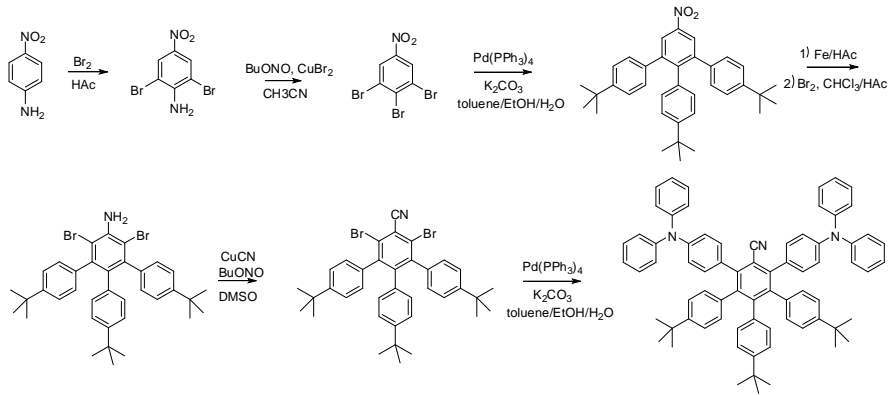


**Chart S2.** Synthetic routes of the synthesis of TPA-CN-TPA.

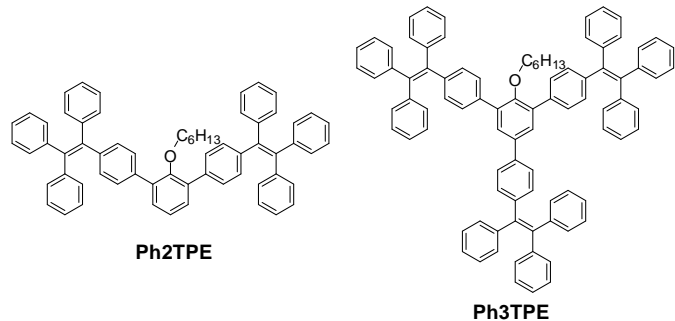
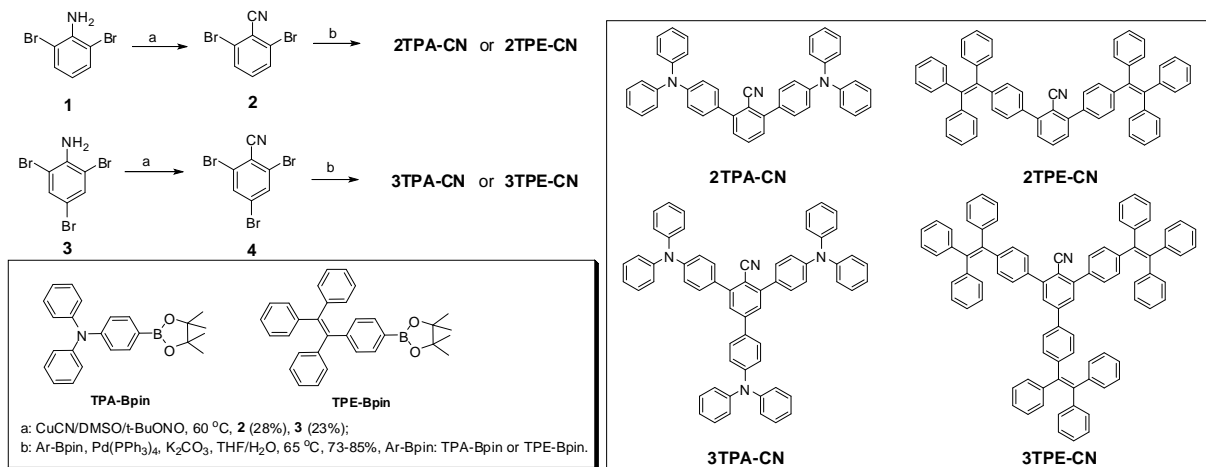


**Chart S3.** Chemical structures of Ph2TPE and Ph3TPE.



**Scheme S1.** Chemical structures and synthetic routes of the previous four luminogens.

### Preparation of compounds:

2,6-Dibromoaniline (**1**) and 2,4,6-tribromoaniline (**3**) were commercial available. All other chemicals and reagents were obtained from commercial sources and used as received without further purification. Solvents for chemical synthesis were purified according to the standard procedures.

*Synthesis of 2,6-dibromobenzonitrile (**2**):* CuCN (117 mg, 1.3 mmol) and **1** (249 mg, 1.0 mmol) was added to a stirred anhydrous DMSO (40 mL) at 50 °C to form a clear solution, then followed by the addition of *tert*-butyl nitrite (0.357 mL, 3.0 mmol). The resultant mixture was allowed to stir for 2 h, then poured into 1 M HCl (100 mL) and extracted with chloroform. The combined organic extracts were dried over anhydrous Na<sub>2</sub>SO<sub>4</sub> and concentrated by rotary evaporation. The crude product was purified by column chromatography on silica gel using chloroform/petroleum ether as eluent to give a pale yellow solid in the yield of 26% (68 mg). <sup>1</sup>H NMR (300 MHz, CDCl<sub>3</sub>) δ (ppm): 7.66-7.64 (d, J = 8.1 Hz, 2H), 7.34-7.31 (m, 1H). <sup>13</sup>C NMR (100 MHz, CDCl<sub>3</sub>) δ (ppm): 134.1, 131.7, 126.7, 118.7, 115.8. MS (EI), m/z: 259.50 ([M<sup>+</sup>], calcd for C<sub>7</sub>H<sub>3</sub>Br<sub>2</sub>N, 258.86). Anal. Calcd for C<sub>7</sub>H<sub>3</sub>Br<sub>2</sub>N: C, 32.22; H, 1.16; N, 5.37. Found: C, 32.36; H, 1.24; N, 5.33.

*Synthesis of 2,4,6-tribromobenzonitrile (**4**):* The synthetic procedure was similar to that of **2**.

**3** (327 mg, 1.0 mmol) reacted with CuCN (117 mg, 1.3 mmol), by the addition of *tert*-butyl nitrite (0.357 mL, 3.0 mmol) to yield **4** (23%, 77 mg, a pale yellow solid). <sup>1</sup>H NMR (300 MHz, CDCl<sub>3</sub>) δ (ppm): 7.61 (s, 2H). <sup>13</sup>C NMR (100 MHz, CDCl<sub>3</sub>) δ (ppm): 134.6, 128.1, 127.0, 117.8, 115.4. MS (EI), m/z: 338.49 ([M<sup>+</sup>], calcd for C<sub>7</sub>H<sub>2</sub>Br<sub>3</sub>N, 336.77). Anal. Calcd for C<sub>7</sub>H<sub>2</sub>Br<sub>3</sub>N: C, 24.74; H, 0.59; N, 4.12. Found: C, 24.99; H, 0.73; N, 4.27.

### Typical Procedure for the Synthesis of Luminogens.

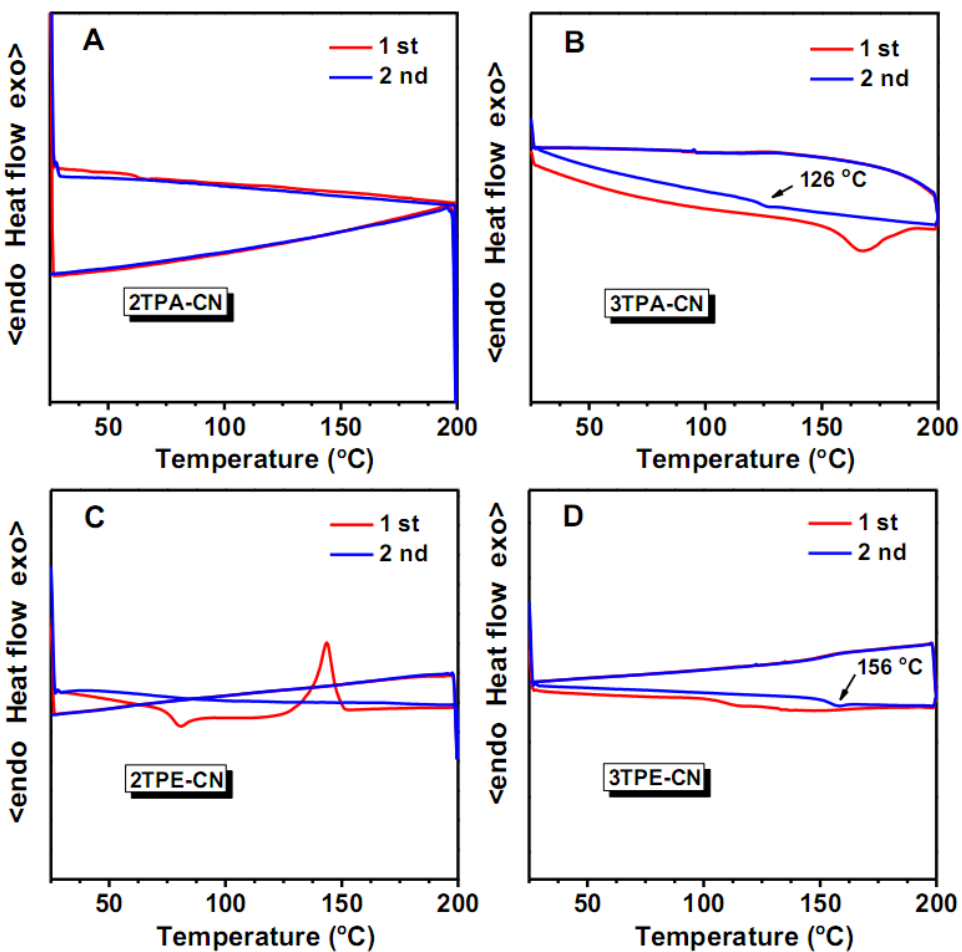
*Synthesis of 2TPA-CN:* A mixture of 2,6-dibromobenzonitrile (103 mg, 0.4 mmol), 4-Bpin-triphenylamine (0.74 g, 2.0 mmol), Pd(PPh<sub>3</sub>)<sub>4</sub> (30 mg) and potassium carbonate (1.10 g, 8.0 mmol) in toluene (8.0 mL), EtOH (2.0 mL) and distilled water (4.0 mL), was refluxed for 24 h under nitrogen in a 100 mL Schlenk tube. After quenched by water, the mixture was extracted with chloroform. The combined organic extracts were dried over anhydrous Na<sub>2</sub>SO<sub>4</sub> and concentrated by rotary evaporation. The crude product was purified by column chromatography on silica gel using chloroform/petroleum ether as eluent to afford the product as white solid in the yield of 76% (179 mg). <sup>1</sup>H NMR (300 MHz, CDCl<sub>3</sub>) δ (ppm): 7.62-7.58 (m, 1H), 7.46-7.40 (m, 6H), 7.32-7.29 (m, 8H), 7.19-7.13 (m, 12H), 7.09-7.04 (m, 4H). <sup>13</sup>C NMR (100 MHz, CDCl<sub>3</sub>) δ (ppm): 148.2, 147.3, 146.6, 132.1, 131.8, 129.8, 129.3, 128.1, 125.0, 123.4, 122.2, 118.4, 109.4. MS (EI), m/z: 589.68 ([M<sup>+</sup>], calcd for C<sub>43</sub>H<sub>31</sub>N<sub>3</sub>, 589.25). Anal. Calcd for C<sub>43</sub>H<sub>31</sub>N<sub>3</sub>: C, 87.58; H, 5.30; N, 7.13. Found: C, 87.32; H, 5.53; N, 7.02.

*Synthesis of 3TPA-CN.* The synthetic procedure was similar to that of **2TPA-CN**. 2,4,6-tribromobenzonitrile (101 mg, 0.3 mmol) reacted with 4-Bpin-triphenylamine (550 mg, 1.5 mmol), in the presence of Pd(PPh<sub>3</sub>)<sub>4</sub> (30 mg) and potassium carbonate (1.24 g, 9.0 mmol), to yield **3TPA-CN** (70%, 174 mg, a pale yellow solid). <sup>1</sup>H NMR (300 MHz, CDCl<sub>3</sub>) δ (ppm): 7.60 (s, 2H), 7.51-7.48 (m, 6H), 7.32-7.30 (m, 10H), 7.19-7.13 (m, 20H), 7.10-7.05 (m, 6H). <sup>13</sup>C NMR (100 MHz, CDCl<sub>3</sub>) δ (ppm): 148.4, 148.2, 147.3, 147.2, 147.0, 144.3, 132.3, 132.0, 129.8, 129.3, 128.0, 126.2, 125.0, 124.8, 123.4, 123.0, 122.3, 118.7, 107.4. MS (EI), m/z: 832.52 ([M<sup>+</sup>], calcd for C<sub>61</sub>H<sub>44</sub>N<sub>4</sub>, 832.36). Anal. Calcd for C<sub>61</sub>H<sub>44</sub>N<sub>4</sub>: C, 87.95; H, 5.32; N,

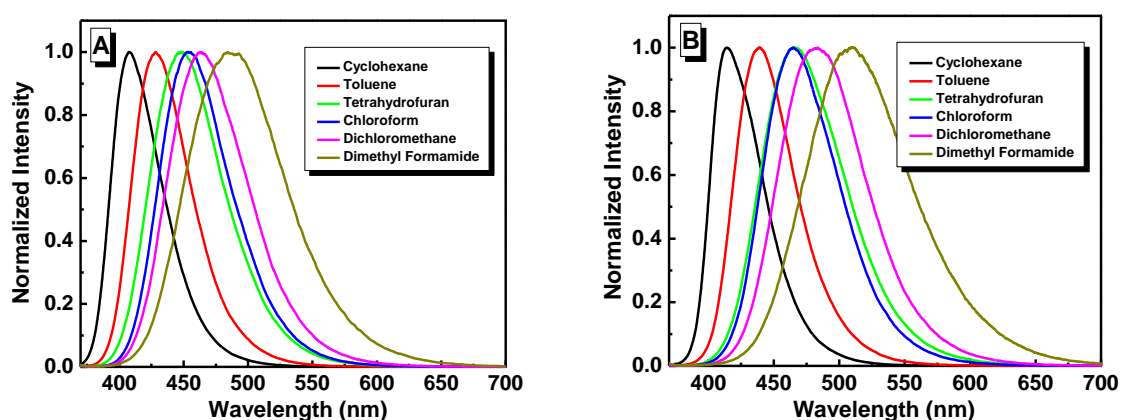
6.73. Found: C, 87.73; H, 5.57; N, 6.61.

*Synthesis of 2TPE-CN.* The synthetic procedure was similar to that of **2TPA-CN**. 2,6-dibromobenzonitrile (259 mg, 1.0 mmol) reacted with 4-Bpin-tetraphenylethene (1.37 g, 3.0 mmol), in the presence of Pd(PPh<sub>3</sub>)<sub>4</sub> (30 mg) and potassium carbonate (2.76 g, 20 mmol) to yield **2TPE-CN** (74%, 563 mg, a light yellow solid). <sup>1</sup>H NMR (300 MHz, CDCl<sub>3</sub>) δ (ppm): 7.60 (m, 1H), 7.39-7.37 (d, J = 7.5 Hz, 2H), 7.31-7.28 (m, 4H), 7.14-7.05 (m, 34H). <sup>13</sup>C NMR (100 MHz, CDCl<sub>3</sub>) δ (ppm): 146.5, 144.0, 143.5, 141.7, 140.2, 136.6, 131.9, 131.4, 131.3, 128.5, 128.2, 128.0, 127.7, 127.6, 127.5, 126.6, 126.5, 117.6, 110.1. MS (EI), m/z: 763.81 ([M<sup>+</sup>], calcd for C<sub>59</sub>H<sub>41</sub>N, 763.32). Anal. Calcd for C<sub>59</sub>H<sub>41</sub>N: C, 92.76; H, 5.41; N, 1.83. Found: C, 92.96; H, 5.70; N, 1.96.

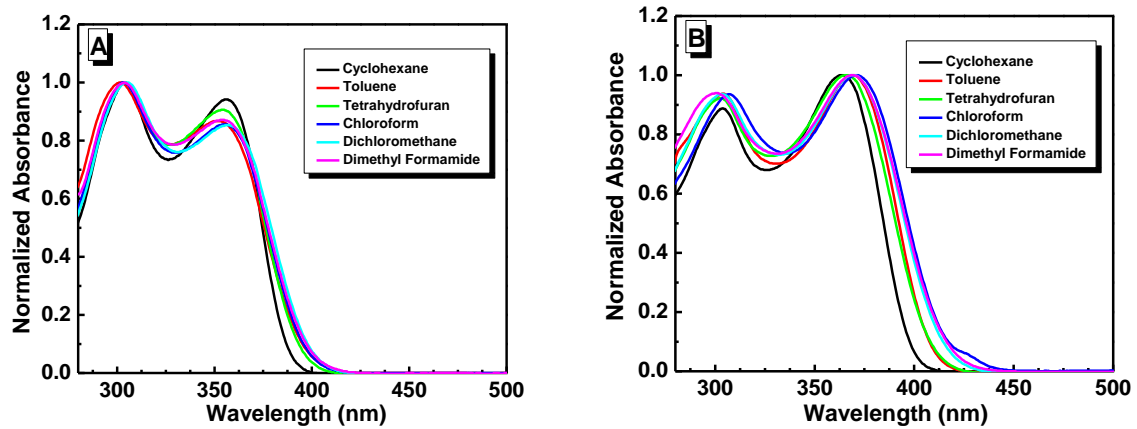
*Synthesis of 3TPE-CN.* The synthetic procedure was similar to that of **2TPA-CN**. 2,4,6-tribromobenzonitrile (168 mg, 0.50 mmol) reacted with 4-Bpin-tetraphenylethene (1.14 g, 2.5 mmol), in the presence of Pd(PPh<sub>3</sub>)<sub>4</sub> (30 mg) and potassium carbonate (2.07 g, 15 mmol) to yield **3TPE-CN** (71%, 387 mg, yellow solid). <sup>1</sup>H NMR (300 MHz, CDCl<sub>3</sub>) δ (ppm): 7.54 (s, 2H), 7.40-7.37 (d, J = 8.1 Hz, 2H), 7.33-7.30 (d, J = 8.7 Hz, 4H), 7.12-7.06 (m, 51H). <sup>13</sup>C NMR (100 MHz, CDCl<sub>3</sub>) δ (ppm): 146.9, 144.3, 144.2, 144.1, 143.5, 143.4, 143.3, 141.7, 140.2, 140.0, 136.6, 132.0, 131.8, 131.7, 131.4, 131.3, 131.2, 128.2, 128.1, 128.0, 127.9, 127.8, 127.7, 127.6, 126.8, 126.7, 126.6, 126.4, 117.8, 108.6. MS (MALDI-TOF), m/z: 1093.37 ([M<sup>+</sup>], calcd for C<sub>85</sub>H<sub>59</sub>N, 1093.46). Anal. Calcd for C<sub>85</sub>H<sub>59</sub>N: C, 93.29; H, 5.43; N, 1.28. Found: C, 93.06; H, 5.46; N, 1.33.



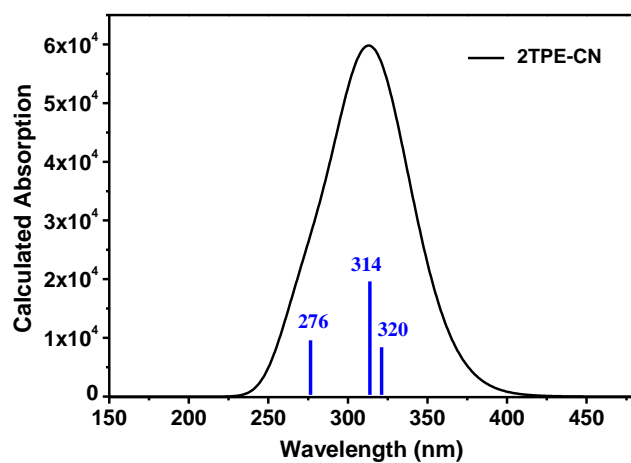
**Figure S1.** DSC curves of the four luminogens recorded under  $N_2$  at a heating rate of 10  $^{\circ}C/min.$  (A: 2TPA-CN; B: 3TPA-CN; C: 2TPE-CN; D: 3TPE-CN)



**Figure S2.** PL spectra of 2TPA-CN (A) and 3TPA-CN (B) in various solvents ( $\sim 10 \mu M$ ).



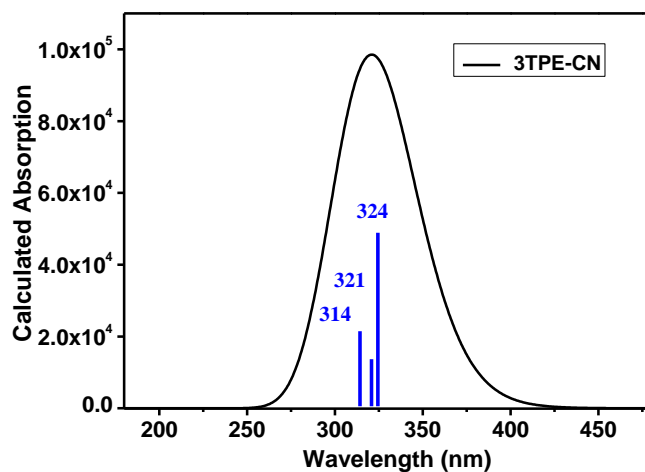
**Figure S3.** UV-vis spectra of **2TPA-CN** (A) and **3TPA-CN** (B) in various solvents ( $\sim 10 \mu\text{M}$ ).



**Figure S4.** Calculated UV spectrum of **2TPE-CN**.

**Table S1.** Absorption wavelengths and oscillator strength of **2TPE-CN** evaluated by the TD-DFT (CAM-B3LYP/6-31G (d)) calculation.

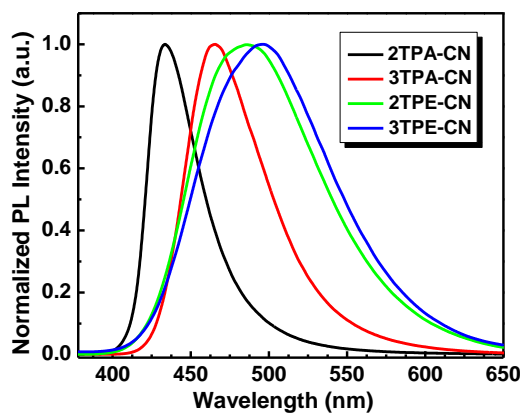
Excitation energies	Absorption[nm] (oscillator strength)	Assignments (%)
3.87 eV	320.07 (0.42)	HOMO-1→LUMO+1 (41)
		HOMO→LUMO (41)
		HOMO→LUMO+2 (10)
3.95 eV	313.67 (0.99)	HOMO-1→LUMO (34)
		HOMO-1→LUMO+2 (15)
		HOMO→LUMO+1 (44)
4.49 eV	276.02 (0.47)	HOMO-2→LUMO (22)
		HOMO→LUMO (17)
		HOMO→LUMO+2 (29)



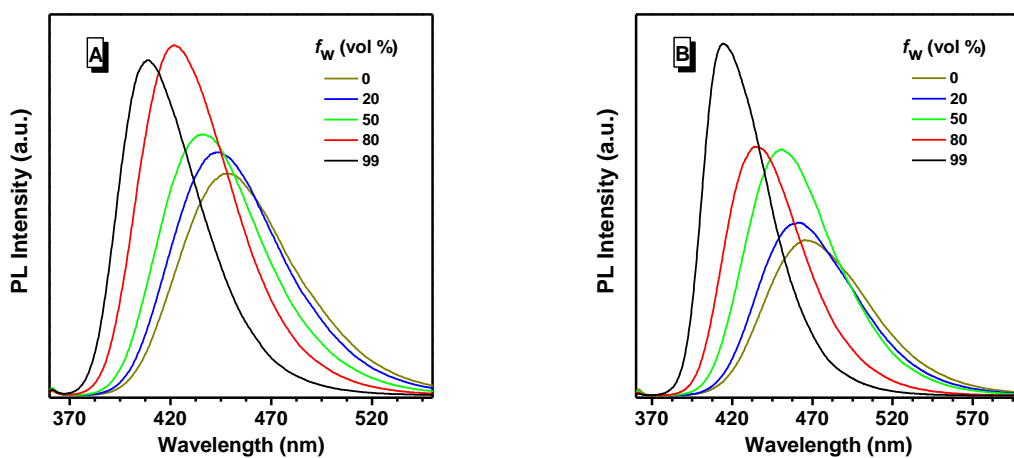
**Figure S5.** Calculated UV spectrum of **3TPE-CN**.

**Table S2.** Absorption wavelengths and oscillator strength of **3TPE-CN** evaluated by the TD-DFT (B3LYP/6-311G (d, p)) calculation.

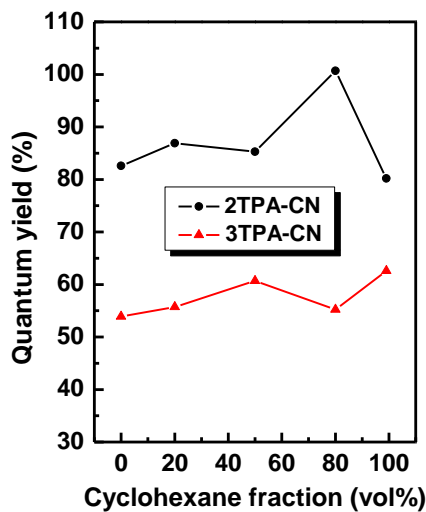
Excitation energies	Absorption[nm] (oscillator strength)	Assignments (%)
3.83 eV	323.86 (1.44)	HOMO-2→LUMO (54) HOMO-2→LUMO+2 (17) HOMO-2→LUMO+3 (11) HOMO-1→LUMO+2 (6) HOMO→LUMO+1 (3)
3.86 eV	321.27 (0.38)	HOMO-1→LUMO+1 (35) HOMO→LUMO (23) HOMO→LUMO+2 (24)
3.95 eV	314.16 (0.64)	HOMO-1→LUMO (19) HOMO-1→LUMO+2 (19) HOMO→LUMO+1 (41)



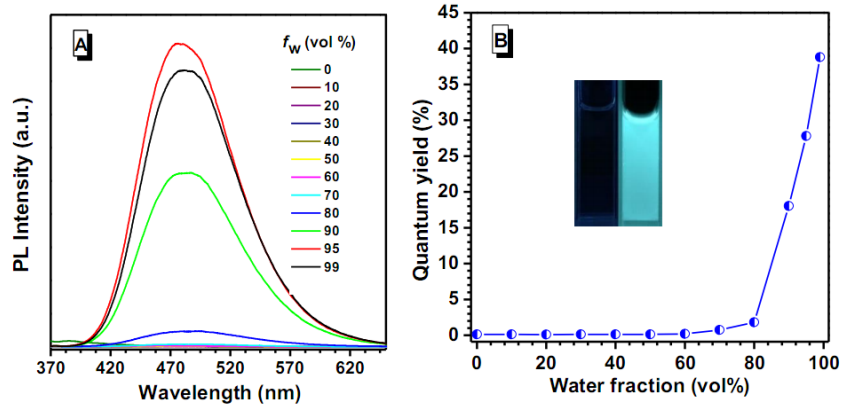
**Figure S6.** PL spectra of the films.



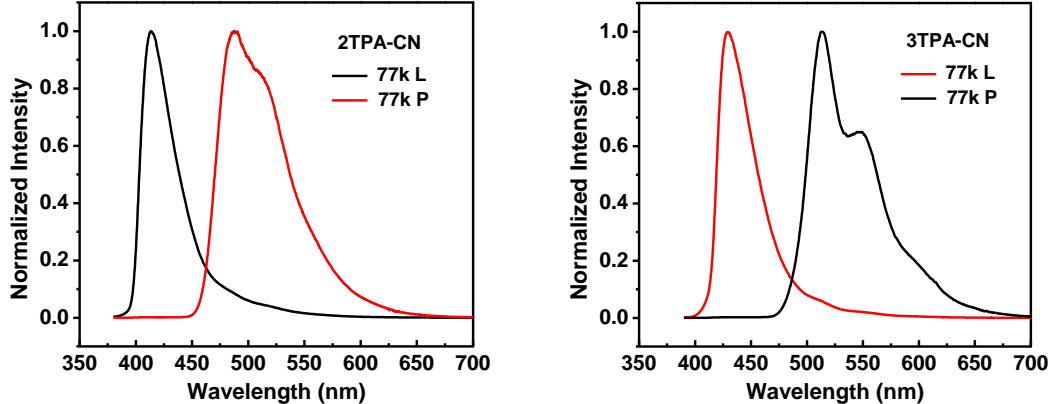
**Figure S7.** PL spectra of **2TPA-CN** (A) and **3TPA-CN** (B) in THF/cyclohexane mixtures with different cyclohexane fractions. Concentration:  $\sim 10 \mu\text{M}$ .



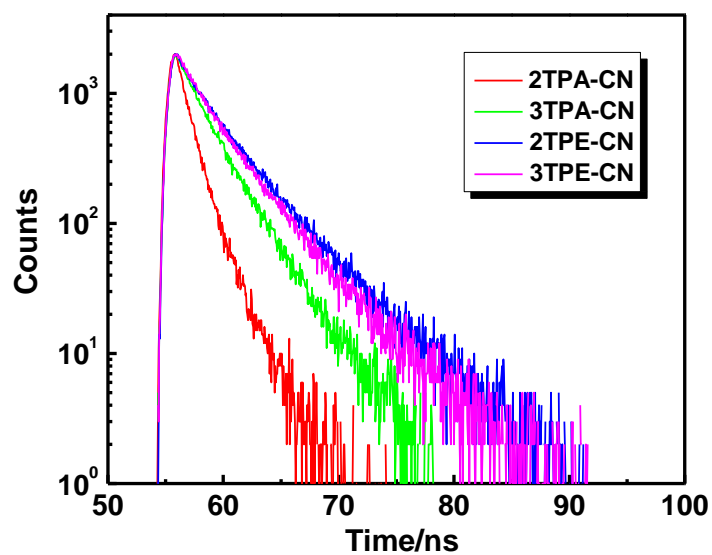
**Figure S8.** Quantum yields of **2TPA-CN** and **3TPA-CN** in THF/cyclohexane mixtures with different cyclohexane fractions.



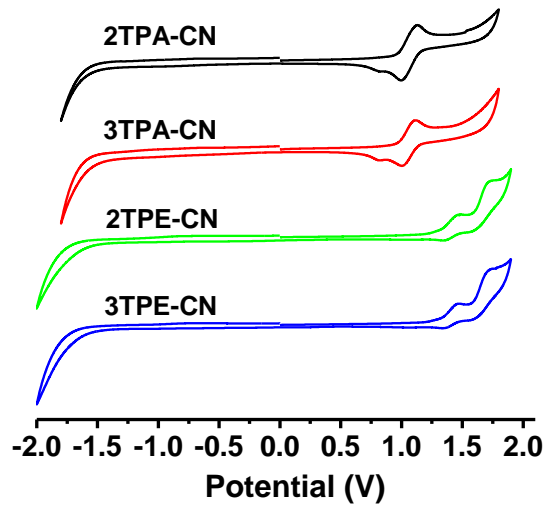
**Figure S9.** (A) PL spectra of **2TPE-CN** in THF/H<sub>2</sub>O mixtures with different water fractions (*f*<sub>w</sub>). (B) Plots of fluorescence quantum yields determined in THF/H<sub>2</sub>O solutions using 9,10-diphenylanthracene ( $\Phi = 90\%$  in cyclohexane) as standard versus water fractions. Inset in (B): photos of **2TPE-CN** in THF/water mixtures (*f*<sub>w</sub>=0 and 99%) taken under the illumination of a 365 nm UV lamp.



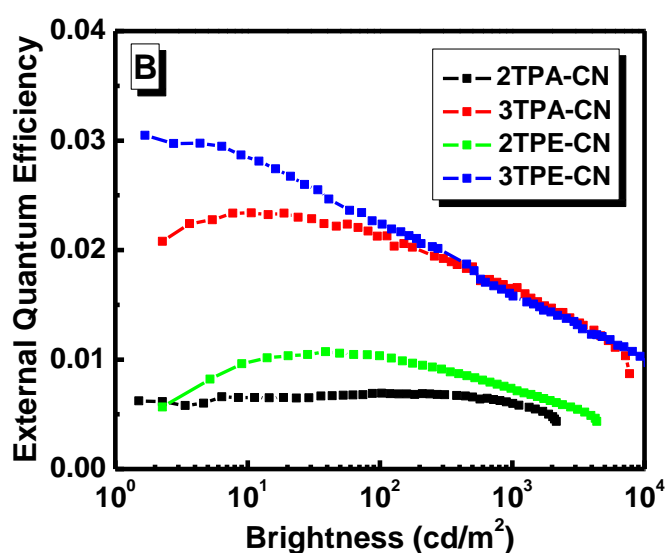
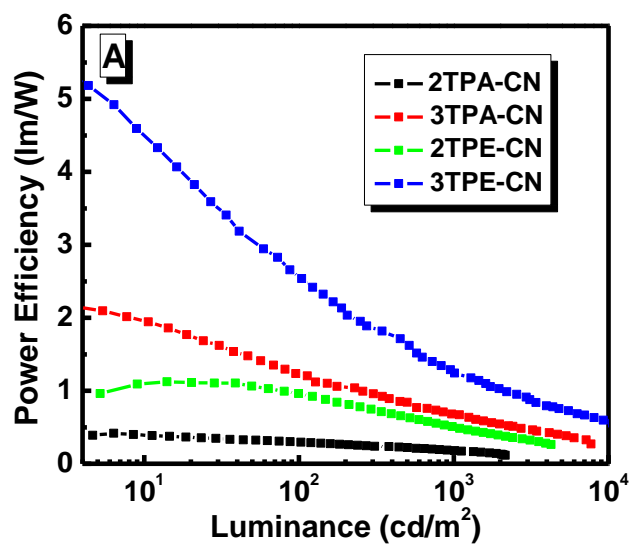
**Figure S10.** Luminescence (L) and phosphorescence (P) spectra of **2TPA-CN** and **3TPA-CN** at 77 K in a frozen 2-methyl-THF matrix. Concentration:  $\sim 10^{-3}$  M.



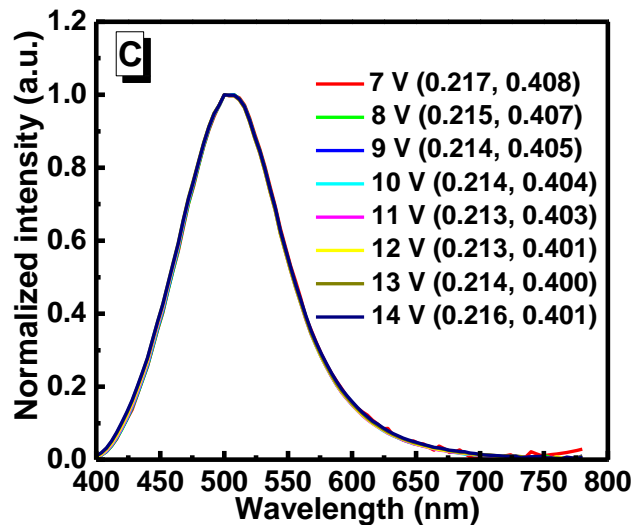
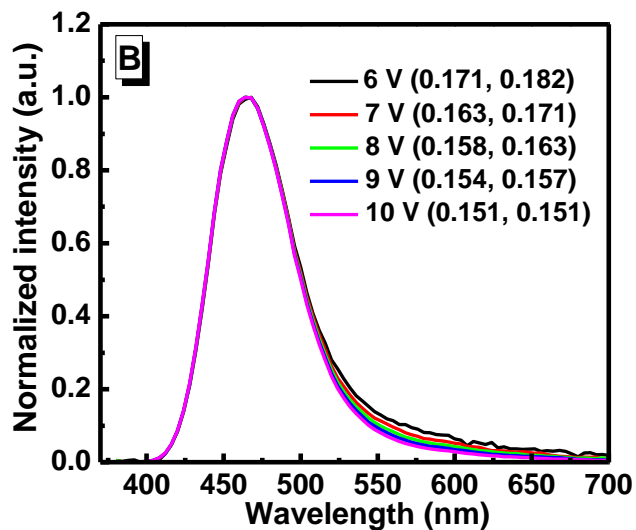
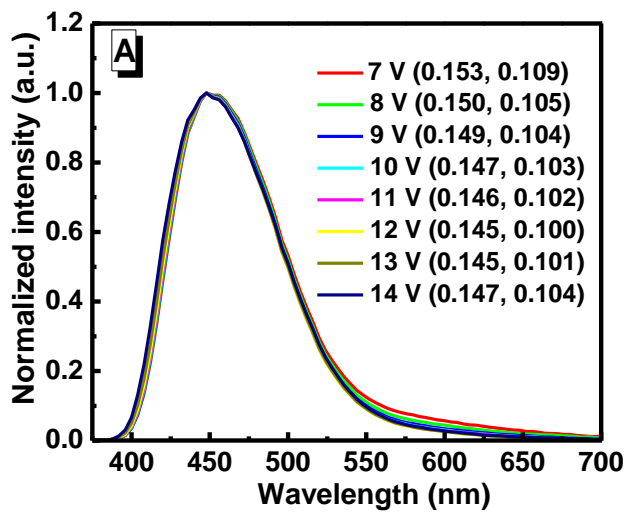
**Figure S11.** Emission decay of the four luminogens in oxygen-free toluene solution at room temperature.

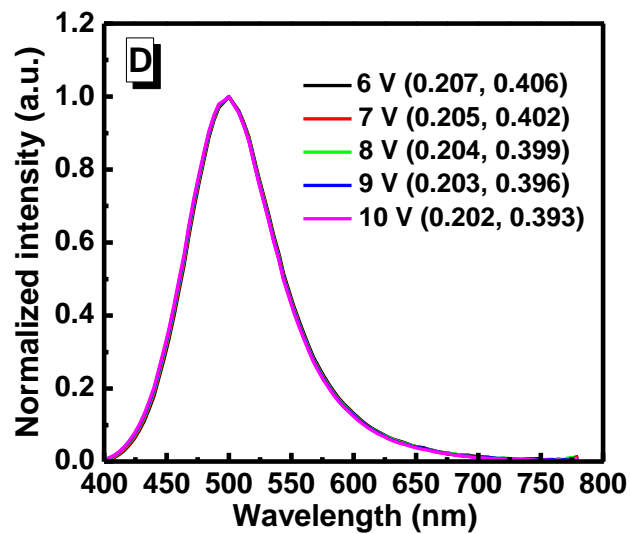


**Figure S12.** Cyclic voltammograms recorded in dichloromethane.

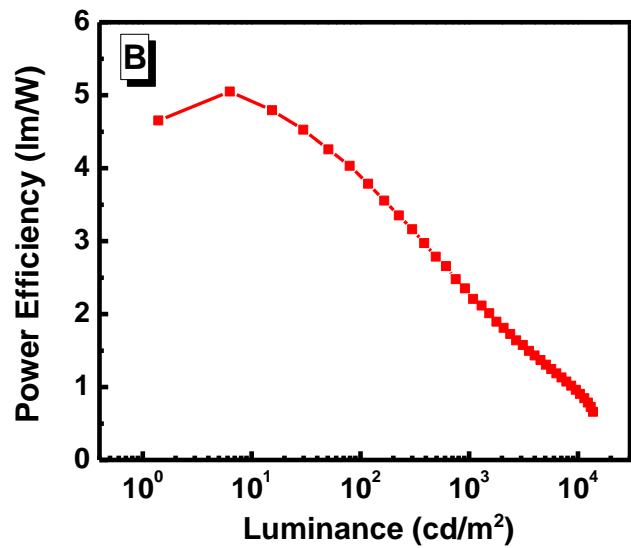
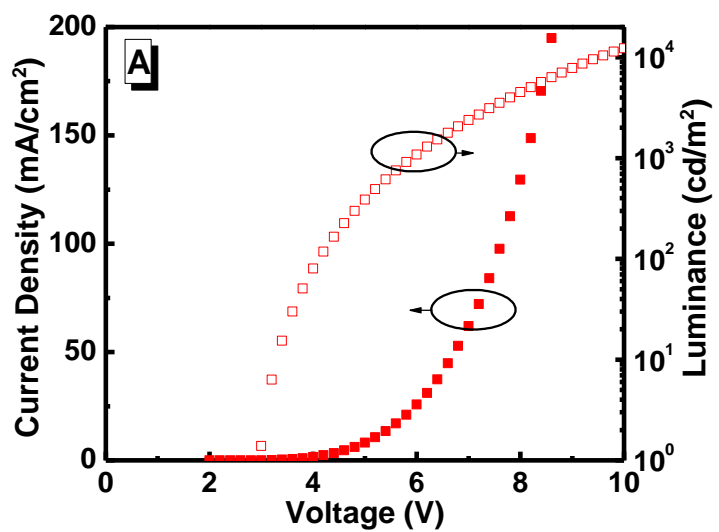


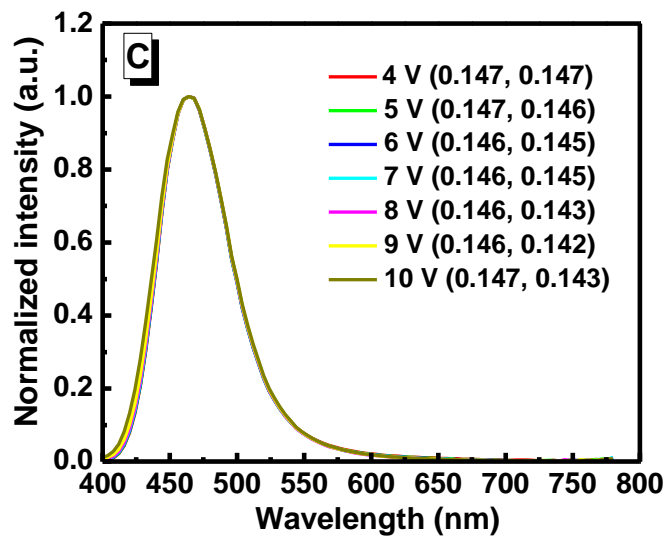
**Figure S13.** (A) Power efficiency-luminance characteristics and (B) External quantum efficiency-luminance characteristics of the four luminogens. Device configurations: ITO / MoO<sub>3</sub> (10 nm) / NPB (60 nm) / mCP (15 nm)/ X (30 nm) / TPBi (30 nm) / LiF (1 nm) / Al.



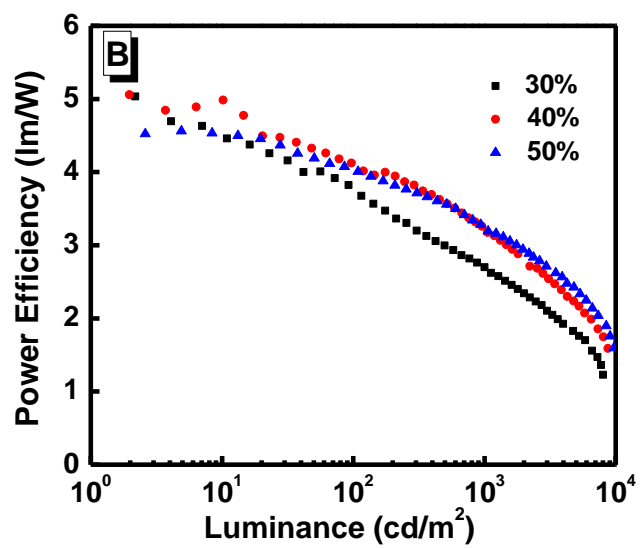
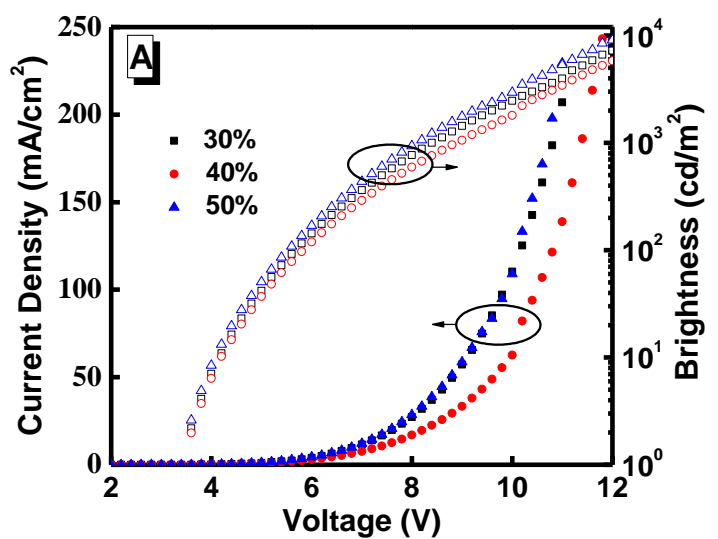


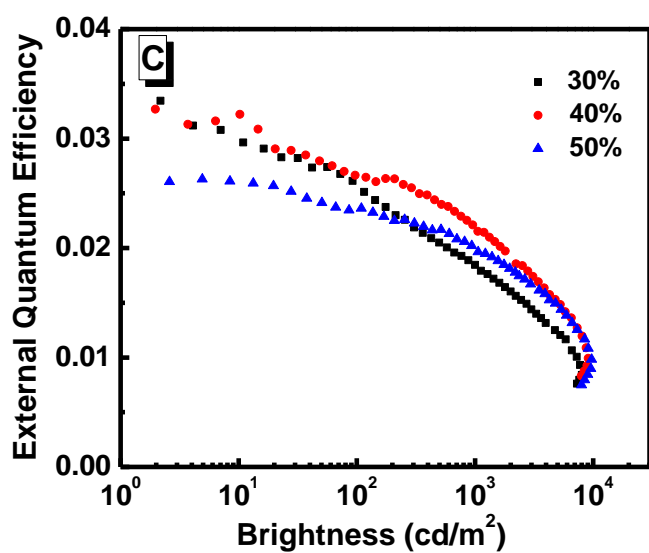
**Figure S14.** EL spectra of EL devices at different applied voltages of **2TPA-CN** (A), **3TPA-CN** (B), **2TPE-CN** (C) and **3TPE-CN** (D). Device configurations: ITO / MoO<sub>3</sub> (10 nm) / NPB (60 nm) / mCP (15 nm)/ X (30 nm) / TPBi (30 nm) / LiF (1 nm) / Al.



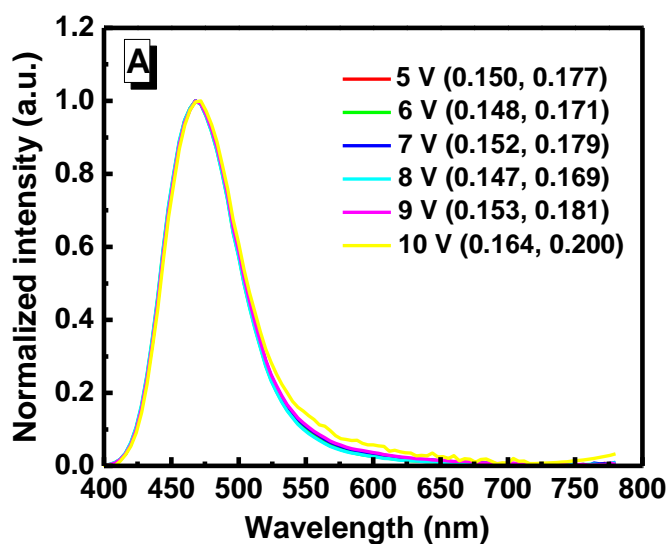


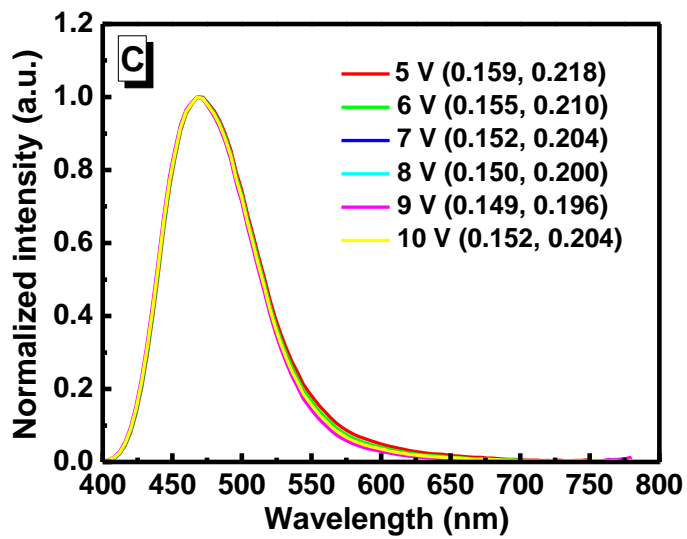
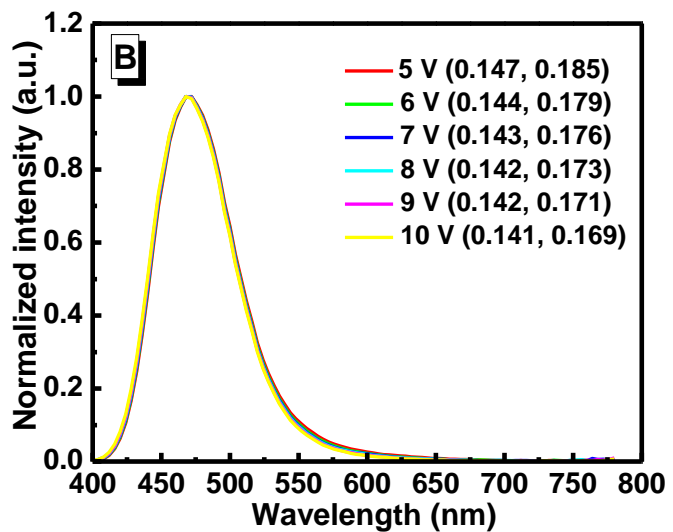
**Figure S15.** (A) Current density-voltage-luminance characteristics, (B) Power efficiency-luminance characteristics and (C) EL spectra of EL device at different applied voltages. Device configurations: ITO / MoO<sub>3</sub> (10 nm) / 3TPA-CN (70 nm) / TPBi (30 nm) / LiF (1 nm) / Al.



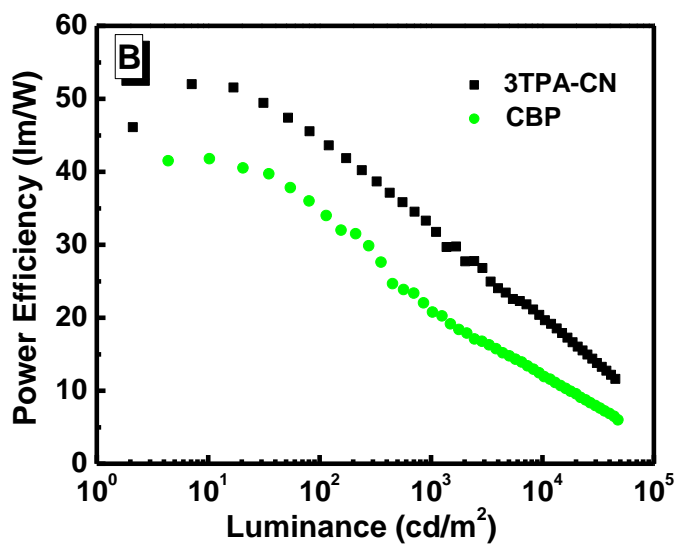
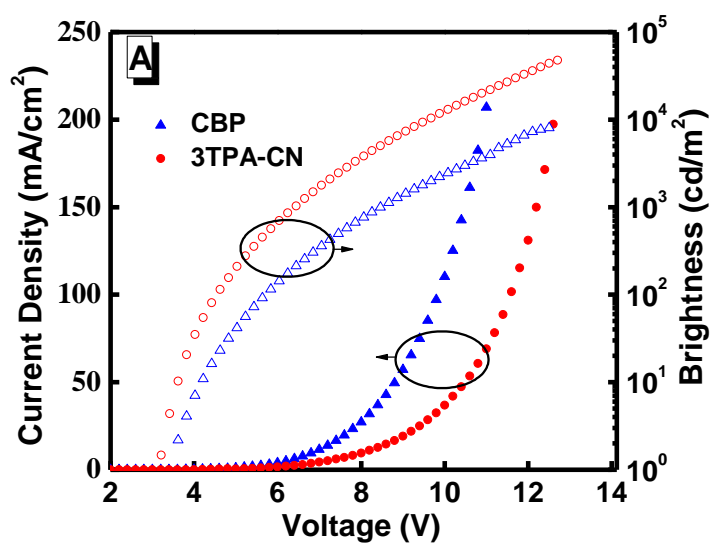


**Figure S16.** (A) Current density-voltage-luminance characteristics, (B) Power efficiency-luminance characteristics and (C) External quantum efficiency-luminance characteristics. Device configurations: ITO / MoO<sub>3</sub> (10 nm) / NPB (60 nm) / mCP (10 nm) / BmPyPb: x% 3TPA-CN (20 nm) / BmPyPb (10 nm) / TPBi (35 nm) / LiF (1 nm) / Al.





**Figure S17.** EL spectra of doped devices at different applied voltages. Device configurations: ITO / MoO<sub>3</sub> (10 nm) / NPB (60 nm) / mCP (10 nm) / BmPyPb: x% **3TPA-CN** (20 nm) / BmPyPb (10 nm) / TPBi (35 nm) / LiF (1 nm) / Al. (A: 30%; B: 40%; C: 50%)



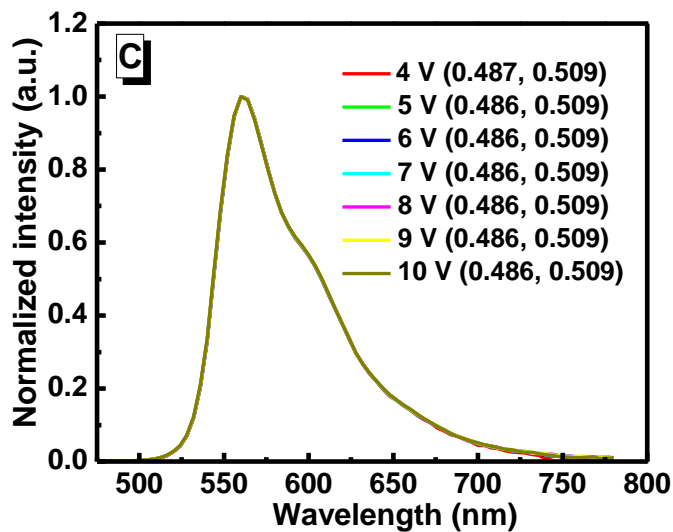


**Figure S18.** (A) Current density-voltage-luminance characteristics, (B) Power efficiency-luminance characteristics and (C) EL spectra of the device with CBP as the host. Device configurations: ITO / MoO<sub>3</sub> / NPB (60 nm) / mCP (10 nm) / CBP:PO-01 (20 nm, 10 wt%) / TPBI (40 nm) / LiF (1 nm) / Al.